

Entanglement spectrum of random-singlet quantum critical points

Maurizio Fagotti,¹ Pasquale Calabrese,¹ and Joel E. Moore^{2,3}

¹*Dipartimento di Fisica dell'Università di Pisa and INFN, Pisa, Italy*

²*Department of Physics, University of California, Berkeley, California 94720, USA*

³*Materials Sciences Division, Lawrence Berkeley National Laboratory, Berkeley, California 94720, USA*

(Received 13 September 2010; revised manuscript received 19 November 2010; published 31 January 2011)

The entanglement spectrum (i.e., the full distribution of Schmidt eigenvalues of the reduced density matrix) contains more information than the conventional entanglement entropy and has been studied recently in several many-particle systems. We compute the disorder-averaged entanglement spectrum in the form of the disorder-averaged moments $\overline{\text{Tr} \rho_A^\alpha}$ of the reduced density matrix ρ_A for a contiguous block of many spins at the random-singlet quantum critical point in one dimension. The result compares well in the scaling limit with numerical studies on the random XX model and is also expected to describe the (interacting) random Heisenberg model. Our numerical studies on the XX case reveal that the dependence of the entanglement entropy and spectrum on the geometry of the Hilbert space partition is quite different than for conformally invariant critical points.

DOI: 10.1103/PhysRevB.83.045110

PACS number(s): 64.70.Tg, 03.67.Mn, 75.10.Pq, 74.62.En

I. INTRODUCTION

The ground state of a system at a quantum critical point shows universal behavior in many quantities. Correlation functions, for example, show universal power-law behavior, and in some cases these power laws can be obtained exactly by mapping the quantum critical point to a system in one more dimension. The most powerful example of this mapping is for one-dimensional (1D) quantum critical points (QCP's) that become two-dimensional (2D) classical critical points with conformal invariance. In addition to standard correlation functions, it is now understood that the entanglement entropy, reviewed in the following (see the comprehensive reviews in Ref. 1), is universal at such quantum critical points and determined by the central charge of the associated 2D conformal field theory.²⁻⁵ For a partition of an infinite 1D system into a finite chain of length ℓ and the remainder, the entanglement entropy (the von Neumann entropy of the reduced density matrix ρ_A) for ℓ much larger than the short-distance cutoff a is asymptotically

$$S_{VN} \equiv -\text{Tr}[\rho_A \ln \rho_A] = \frac{c}{3} \ln \frac{\ell}{a} + c'_1, \quad (1)$$

where c is the central charge and c'_1 a nonuniversal additive constant.

Other properties related to entanglement are less well understood, even at these quantum critical points, such as the entanglement spectrum (the full set of reduced density matrix eigenvalues) and the full set of entanglement Renyi entropies; one exception is free Fermi models, where the entanglement spectrum is given by the spectrum of an effective “entanglement Hamiltonian”.⁶ A form for the spectrum⁷ at 1D conformal QCP's that is exact in some cases and a good approximation in others^{8,9} can be used to develop a theory of how finite entanglement perturbs criticality in numerical studies.^{10,11} The entanglement spectrum has also been applied to understanding gapped (noncritical) topological phases,¹²⁻¹⁴ where it contains information about the edge excitation spectrum that goes beyond the universal constant in the entanglement entropy.¹⁵⁻¹⁷ The same is true for quantum 2D models with conformal invariant ground-state wave

functions.¹⁸ Also results for a critical nonconformal 1D model are available.¹⁹

This paper studies the entanglement spectrum at “random-singlet” 1D QCP's in which quenched disorder leads to a renormalization group (RG) flow to infinite randomness. We obtain the disorder-averaged moments of the Schmidt eigenvalue distribution analytically and compare them to numerical results on a special case with a free-fermion representation, the random XX model. While these critical points are not conformally invariant (after mapping to a 2D problem, the imaginary-time direction has no randomness and is hence very different from the spatial direction), their disorder-averaged correlation functions have nevertheless been understood in many cases²⁰⁻²² by real-space renormalization group method.²³ The entanglement entropy at random-singlet critical points was already known²⁴⁻²⁸ to show universal behavior similar to that at 1D conformal QCP's [Eq. (1)], with a modified prefactor of the logarithm (analogous to c) that was initially viewed as an effective central charge for random systems.

However, the results presented here indicate that this similarity does not extend to the full entanglement spectra, which are rather different. We start by considering the disorder-averaged Renyi entropies

$$S_\alpha = \frac{1}{1-\alpha} \overline{\ln \text{Tr}[\rho_A^\alpha]}, \quad (2)$$

where the bar denotes the average over quenched disorder. These Renyi entropies S_α are quite simple in the random-singlet phase: They depend only on the mean number of singlets across the partition used to define the entanglement, just as does the entanglement entropy. The Renyi entropies already behave differently than in the conformal case. However, in disordered systems S_α is not the right quantity that determines the entanglement spectrum via Laplace transform in α (Ref. 7). To obtain the averaged moments of the distribution, one should instead consider the entropies corresponding to averaging the disorder *before* taking the logarithm

$$\hat{S}_\alpha = \frac{1}{1-\alpha} \ln \overline{\text{Tr}[\rho_A^\alpha]}. \quad (3)$$

This definition has also the advantage to maintain the relationship of the pure system between the Tsallis²⁹ entropies $(\text{Tr}[\rho_A^\alpha] - 1)/(1 - \alpha)$ and the Rènyi entropies. These moments of the entanglement eigenvalue distribution reveal the full distribution of the number of singlets crossing a boundary and require an improved calculation. Both generalized entropies reduce to the Von Neumann one for $\alpha \rightarrow 1$

$$S_{VN} = \lim_{\alpha \rightarrow 1} S_\alpha = \lim_{\alpha \rightarrow 1} \hat{S}_\alpha. \quad (4)$$

The entropies S_α and \hat{S}_α together with other properties are then studied for the random XX model and the validity of our results is discussed for general random-singlet ground states. The paper is organized as follows. In Sec. II we present the random-singlet picture and we derive the entropies S_α within strong disorder renormalization group. In Sec. III we introduce the probability distribution of singlet formation and use it to derive the entropies \hat{S}_α . Numerical tests of the predicted entropies and the discussion of their universality are described in Sec. IV. Finally, in Sec. V, we report our main conclusions.

II. RANDOM-SINGLET PICTURE OF THE RENYI ENTROPIES

The ground state of a strongly disordered $s = 1/2$ Heisenberg chain or of the disordered XX chain

$$H = \frac{1}{4} \sum_l^L J_l (\sigma_l^x \sigma_{l+1}^x + \sigma_l^y \sigma_{l+1}^y), \quad (5)$$

is described by the random-singlet phase (RSP) for essentially any probability distribution $P(J)$ of the coupling. When a system reaches this phase the ground state becomes almost factorized in singlets between spins at arbitrary large distances. The configuration of the singlets depends on the coupling constants J_l , but several universal properties emerge in the average over disorder that are independent of the disorder distribution itself. The physical properties of a system in the RSP can be attained in an indirect way [i.e., without referring (manifestly) to the particular Hamiltonian]. The real-space renormalization group approach (RSRG) is based on the picture that the strongest bond gives rise to a singlet and the near-neighborhood spins can be described by means of an effective interaction from second-order perturbation theory.

Considering the XX Hamiltonian (5), the Ma-Dasgupta rule²⁰ for the effective coupling constant after a decimation (i.e., the formation of a singlet) is

$$(\dots, J_l, J_M, J_r, \dots)_L \rightarrow \left(\dots, \frac{J_l J_r}{J_M}, \dots \right)_{L-2}, \quad (6)$$

where J_M is the strongest bond of the chain of size L and J_l (J_r) is the near-neighborhood left (right) coupling constant. One of the most important consequences of Eq. (6) is that the distribution of the couplings after a sufficiently large number of decimations m with

$$\beta_i^{(m)} = \ln \frac{J_M^{(m)}}{J_i^{(m)}}, \quad (7)$$

is substantially independent of the initial distribution

$$P(\beta) = \frac{1}{\Gamma(m)} e^{-\frac{\beta}{\Gamma(m)}}, \quad (8)$$

where Γ is the RG flow parameter $\Gamma^{(m)} = \ln \frac{J_M^{(0)}}{J_M^{(m)}}$. The distribution (8) is the key to the physical characteristics of the random-singlet phase. It is also the main ingredient for investigating the entanglement of spin blocks. In fact, for a spin block of length ℓ in a given RSP configuration with n singlets linking the spins inside the subsystem with the spins outside (which we call in-out singlets) the reduced density matrix is

$$\rho_A^{\text{RSP}} \sim \bigotimes_{j=1}^n \begin{pmatrix} \frac{1}{2} & 0 \\ 0 & \frac{1}{2} \end{pmatrix} \bigotimes_{j=1}^{\ell-n} \begin{pmatrix} 0 & 0 & 0 & 0 \\ 0 & \frac{1}{2} & -\frac{1}{2} & 0 \\ 0 & -\frac{1}{2} & \frac{1}{2} & 0 \\ 0 & 0 & 0 & 0 \end{pmatrix}. \quad (9)$$

Thus, the entanglement of a subsystem of size ℓ depends only on the mean number \bar{n} of in-out singlets. In particular, the entanglement entropy, as well as any Renyi entropy (2), is proportional to the number of in-out singlets

$$S_\alpha^{\text{RSP}} = \bar{n} \ln 2. \quad (10)$$

(This result has been also discussed in Refs. 28 and 30.) Reference 24 shows that the averaged number of in-out singlets can be deduced directly from the flow equation for the distribution of couplings β_i

$$\frac{dP(\beta)}{d\Gamma} = P(0) \int_0^\infty d\beta_1 \int_0^\infty d\beta_2 \delta_{\beta-\beta_1-\beta_2} \times P(\beta_1)P(\beta_2) + \frac{\partial P(\beta)}{\partial \beta}. \quad (11)$$

After some manipulation, this equation leads to²⁴

$$\bar{n} \simeq \frac{1}{3} \ln \ell, \quad (12)$$

and so the entanglement entropy of a block of length ℓ is

$$S_{VN}^{\text{RSP}}(\ell) \simeq \frac{\ln 2}{3} \ln \ell, \quad (13)$$

with a weight-factor $\frac{\ln 2}{3}$ that calls to mind the behavior in the absence of disorder with an effective central charge $\ln 2$.

Consideration of the Rènyi entropy rather than the standard entanglement entropy suggests that the similarity between the entanglement entropy with and without disorder is only superficial. Indeed in the RSP all Rènyi entropies scale in the same way (10). If we wish to define an effective central charge, we could use any conformal Rènyi entropy⁴

$$S_\alpha^{\text{CFT}}(\ell) = \frac{c}{6} \left(1 + \frac{1}{\alpha} \right) \ln \frac{\ell}{a} + c'_\alpha, \quad (14)$$

as a starting point so that the effective central charge would have any value in the range $[\ln 2, \ln 4]$ while α runs from 1 to infinity. Also the central charge of the clean system $c = 1$ belongs to this range, making questionable any attempt to generalize the Zamolodchikov ‘‘c-theorem’’.³¹ This picture from Rènyi entropy is consistent with the previous counterexamples^{32,33} indicating that there is no version of the c-theorem for entanglement entropy that would describe

the flow from clean to random systems³² or within random systems.³³

The disorder-averaged R enyi entropies at random quantum critical points are universal and already indicate that the RSP's entanglement is quite different from the universal entanglement at 1D conformal QCP's. However, since they depend on the same quantity (mean number \bar{n} of in-out singlets) as the entanglement entropy, they do not probe new features of the random-singlet picture. In the next section we consider additional quantities that are sensitive to new features and directly probe a memory effect in the RSRG flow, or "repulsion between decimations" in RG space, that was a key step in obtaining the correct value of \bar{n} . Numerical tests of the predicted R enyi entropies are described in Sec. IV.

III. GENERALIZED ENTROPY AND THE PROBABILITY DISTRIBUTION OF SINGLET FORMATION

The disorder-averaged Renyi entropy in the RSP only reflects the averaged number of the in-out singlets. Thus it is not a natural measure of the full in-out singlet distribution $P(n)$ or the probability distribution of the Renyi entropy. $P(n)$ can be examined by considering \hat{S}_α in Eq. (3). In fact, denoting with $g(t)$ the cumulant-generating function of the in-out singlet distribution $P(n)$

$$g(t) = \ln\langle e^{nt} \rangle \equiv \ln \sum_{n=0}^{\infty} P(n)e^{nt}, \quad (15)$$

it is straightforward that

$$\hat{S}_\alpha^{\text{RSP}} = \frac{g[t(\alpha)]}{1 - \alpha}, \quad (16)$$

where to keep the notation compact we defined

$$t = t(\alpha) \equiv (1 - \alpha) \ln 2. \quad (17)$$

Throughout the paper t will always denote this quantity, even when the α dependence is not specified. \hat{S}_α does depend on α in the RSP, unlike the R enyi entropy S_α . We require Eq. (15) to not blow up when $n \rightarrow \infty$, and so [assuming a reasonable] we need $t \leq 0$ corresponding to $\alpha \geq 1$. We do not discuss a possible analytic continuation to $\alpha < 1$ (that also in some clean systems can be complicated).³⁴

From the RSRG point of view, singlets form at a constant rate with respect to an "RG time" μ and this rate determines the logarithmic scaling of entanglement entropy. En route to calculating this rate, Ref. 24 obtains the expression for the distribution of waiting times for a decimation across a bond since the last decimation

$$f(\mu) = \frac{1}{\sqrt{5}} \left(e^{-\frac{3-\sqrt{5}}{2}\mu} - e^{-\frac{3+\sqrt{5}}{2}\mu} \right). \quad (18)$$

The above distribution has been deduced neglecting nonuniversal terms coming from the starting disorder distribution: Eq. (18) is only asymptotically true. For example, we expect that the additive constant of the von Neumann entropy S_{VN} should be disorder dependent.

During the RG time between two decimations several processes can happen. The most probable one is the formation of isolated singlets. Considering only this process leads to the

renewal equation

$$\langle e^{nt} \rangle_\mu = \int_0^\infty d\mu' f(\mu') + e^t \int_0^\mu d\mu' f(\mu') \langle e^{nt} \rangle_{\mu-\mu'}. \quad (19)$$

This equation can be solved by the Laplace transformation. Calling $\hat{f}(s)$ the Laplace transform of $f(\mu)$

$$\hat{f}(s) = \frac{1}{\sqrt{5}} \left(\frac{1}{s + \frac{3-\sqrt{5}}{2}} - \frac{1}{s + \frac{3+\sqrt{5}}{2}} \right), \quad (20)$$

we have

$$g_{(\mu)}(t) = \ln \left[\mathcal{L}^{-1} \left\{ \frac{1}{s} \frac{1 - \hat{f}(s)}{1 - e^t \hat{f}(s)} \right\} (\mu) \right], \quad (21)$$

and in particular $\bar{n} = \lim_{t \rightarrow 0^-} g'(t)$.

After simple algebra, we obtain

$$e^{g_{(\mu)}(t)} = \left(\frac{1}{2} + \frac{3}{2\sqrt{5} + 4e^t} \right) e^{-\frac{3-\sqrt{5}+4e^t}{2}\mu} + \left(\frac{1}{2} - \frac{3}{2\sqrt{5} + 4e^t} \right) e^{-\frac{3+\sqrt{5}+4e^t}{2}\mu}, \quad (22)$$

that via Eq. (16) gives \hat{S}_α in the RSP. This is the main analytic result of this paper. It is useful to rewrite it in terms of the mean number of singlets as

$$g(t) = t A_t \bar{n} + t B_t, \quad (23)$$

where the multiplicative t factor is introduced to write more compact formulas for \hat{S}_α via Eq. (16). The two constants A_t and B_t are obtained by plugging Eq. (23) into Eq. (22)

$$\begin{cases} A_t = 3 \frac{\sqrt{5} + 4e^t - 3}{2t}, \\ B_t = \frac{1}{t} \ln \left(\frac{1}{2} + \frac{3}{2\sqrt{5} + 4e^t} \right) + \frac{\sqrt{5} + 4e^t - 3}{6t}. \end{cases} \quad (24)$$

Notice that in Eq. (23) all the dependence of $g_{(\mu)}(t)$ on μ is encoded in \bar{n} . In this way, we also separated the universal $\ln \ell$ behavior (we remind that $\bar{n} \propto \ln \ell$) given by A_t from the constant one B_t . We will come back to the discussion of the universal features of Eqs. (23) and (24) in the next section when comparing with the numerical results.

IV. NUMERICAL RESULTS

In this section we present numerical evidence confirming the critical scaling of the quantities calculated analytically by means of RSRG. We also present results for which we do not have yet any theoretical explanation, like the finite size scaling in the RSP.

The entropies S_α and \hat{S}_α can be directly calculated for the disordered XX chain (5), by generalizing the method of Lafflorencie.²⁵ In fact, for any realization of the disorder (i.e., any distribution of the bonds J_l), the XX model can be mapped into a free-fermionic Hamiltonian by the Jordan-Wigner transformation $c_l^\dagger = \prod_{j<l} \sigma_j^z \sigma_l^+$ that leaves the eigenvalues of the reduced density matrix of a single block unchanged because the transformation is local inside the block. Defining the correlation matrix $C_{ln} = \langle c_l^\dagger c_n \rangle$, the reduced density matrix of a spin block that goes from the site $l_0 + 1$ to $l_0 + \ell$ is the

exponential of a free-fermion operator^{6,35} and it is completely characterized by the $\ell \times \ell$ correlation matrix C in which indexes run from $l_0 + 1$ to $l_0 + \ell$, which we call $C_\ell^{[l_0]}$. The entanglement entropy of the block in this configuration of the disorder is then given by

$$S_{VN}^{[l_0]}(\{J_l\}) = -\text{Tr}[C_\ell^{[l_0]} \ln C_\ell^{[l_0]} + (1 - C_\ell^{[l_0]}) \ln (1 - C_\ell^{[l_0]})], \quad (25)$$

while the Renyi entropy is

$$S_\alpha^{[l_0]}(\{J_l\}) = \frac{1}{1-\alpha} \text{Tr}[\ln((C_\ell^{[l_0]})^\alpha + (1 - C_\ell^{[l_0]})^\alpha)], \quad (26)$$

where we stressed the dependence on the disorder configuration $(\{J_l\})$ and on the first site of the block $l_0 + 1$. Indeed, on a single realization of the disorder, translational invariance is explicitly broken. Only after taking the disorder average translation can symmetry be restored. Having the R enyi entropies for a single realization allows to obtain the asymptotic results for the disordered model by averaging over a large enough number of configurations (generated randomly according to the specific rules for $\{J_l\}$). S_α and \hat{S}_α are obtained by averaging S_α or $e^{(1-\alpha)S_\alpha}$, respectively.

The method we presented is an *ab initio* calculation of the R enyi entropies for disordered spin chains valid every time the model has a free-fermionic representation (as in XX or Ising chains). It is, however, numerically demanding. A more effective numerical technique exploits the RSP structure of the ground state. Starting from a given disorder realization, we construct a singlet where the strong bond lies and we proceed to decimation according to the rule in Eq. (6). We repeat this procedure until we span the entire chain. At this point we are left with a collection of singlets, and then, counting the number of singlets connecting the inside of the block with the outside, we have the configurational R enyi entropies from the relation $S_\alpha^{[l_0]}(\{J_l\}) = n^{[l_0]}(\{J_l\}) \ln 2$. As for the *ab initio* calculation, S_α and \hat{S}_α are obtained by averaging over the disorder. Note that S_α^{RSP} does not depend on α by definition since for any configuration $S_\alpha = \bar{n} \ln 2$. Oppositely, \hat{S}_α depends on α because the average is taken over $e^{(1-\alpha)S_\alpha}$ and indeed some results for \hat{S}_α have been already reported³⁶ by using this method. For completeness, we give few general features for an intuitive picture of the entanglement in the RSP. After a decimation (6), the renormalized bond is strongly suppressed (i.e., singlets repel). The singlets that stay inside the block involve always an even number of spins, thus the parity of the block gives the parity of the number of in-out singlets. The spins belonging to the longest bonds crossing the two ends of the chain can be also thought of as boundaries of two open chains. This suggests that in the RSP (as it is the case for clean systems⁴) the entanglement entropy of a block of ℓ spins in a periodic chain is equivalent to twice the entanglement entropy of $\ell/2$ spins in an open chain with the block starting from the boundary [i.e., $S_\alpha^{\text{periodic}}(\ell) \approx 2S_\alpha^{\text{open}}(\ell/2)$]. However, this argument does not provide information about the additive constant (in clean models, the difference of the two constant terms gives the Affleck and Ludwig boundary entropy).^{4,37,38}

To avoid confusion between the two determinations of the entanglement, in the following we will always refer to the first

method as *ab initio* while to the second as RSP. We stress that the RSP technique can be applied to any model with an RSP ground state, as, for example, the disordered Heisenberg chains or spin-1 chains,²⁷ while the *ab initio* one only to models having a free-fermionic representation. However, the *ab initio* method has the advantage to be exact by definition. Instead, by counting the number of singlets, we make the assumption that the ground state has an RSP structure and that all the universal entanglement physics can be extracted from this. Although both assumptions sound reasonable, it is always worthwhile to perform in parallel the two numerical studies. In fact, the numerical counting of singlets is not the same as the analytic expressions derived in the previous sections because, to provide analytic results, few further assumptions have been made (e.g., considering only the formation of isolated singlets, etc.). In the case of disagreement between formulas and numerics, making the two computations in parallel helps to understand if the error is in the approximations made to solve the equations or in the RSP assumption itself.

A possible generalization (that is currently under investigation³⁹) is to understand if the RSP structure catches the entanglement of two disconnected blocks. This can be achieved by calculating *ab initio* R enyi entropies (indeed there are not known formulas for the entanglement entropy when the subsystem consists of more than one spin block, only some expressions have been recently found for the first integer R enyi entropies⁴⁰) and comparing with the in-out singlets from both blocks. It has been shown for conformal critical models^{40,41} that the entanglement of two blocks provides much more information about the conformal structure than the single block one, and it is then worth investigating this issue also for the random case.

A. Analysis of S_α

We computed *ab initio* the averaged R enyi entropies S_α for many different system sizes. In Fig. 1, we report the result for a chain of $L = 1024$ spins for the disorder average over a sample of 73 000 realizations. For $1 \ll \ell \ll L$, the various curves

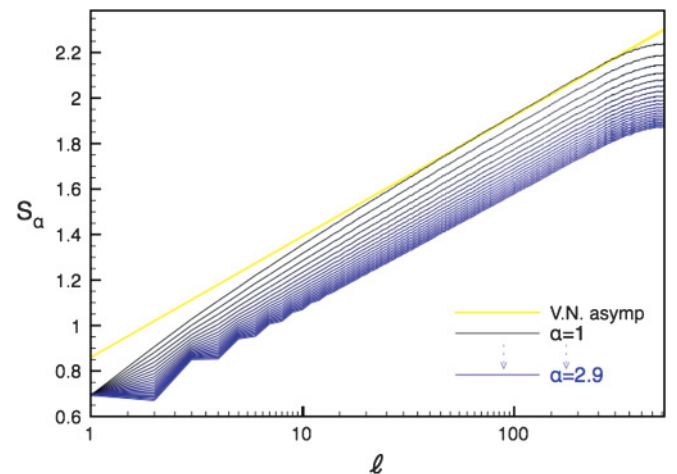


FIG. 1. (Color online) *Ab initio* Renyi entropies for a disordered XX chain of 1024 spins. The average is over 73 000 realizations. The variation of the color shows results from $\alpha = 1$ (upper line) to $\alpha = 2.9$ (bottom line). The yellow line is the asymptotic von Neumann entropy ($\alpha = 1$) obtained by Laflorencie.²⁵

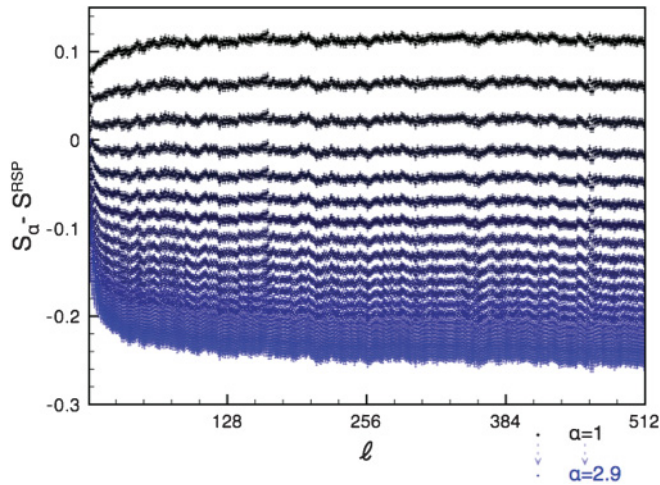


FIG. 2. (Color online) *Ab initio* Rényi entropies for a disordered XX chain of 1024 spins minus the RSP value. The averages are over the same sample of 73 000 realizations.

are parallel, with the slope predicted by Eq. (13) (i.e., the leading term of S_α is α independent). The nonuniversal additive $O(1)$ term clearly depends on α , as in the clean case. On top of a smooth behavior, we can see oscillating contributions, evident for small ℓ and large α . Their presence does not come as unexpected: Also in clean chains^{42–44} there are oscillating terms that (in zero magnetic field) are parity dependent [i.e., they are of the form $(-1)^\ell$]. However, for random systems the oscillations have a different form and they decay rather quickly with ℓ (as opposite to \hat{S}_α as we shall see). We do not have a proper theory for their origin, nor a phenomenological description, but their understanding is beyond the goals of this paper since they do not influence the determination of the asymptotic behavior. When ℓ approaches the chain length L , sizable finite-size corrections are visible. The next section will be devoted to their accurate study, while here we continue with the asymptotic analysis of S_α .

We compare the data in Fig. 1 from the *ab initio* calculation with the numerical results obtained using the RSP approach on the same random sample of 73 000 realizations of J_I . According to Eq. (10), the RSP Rényi entropies do not depend on α by definition. For this reason, in Fig. 2 we report the difference between the RSP Rényi entropies and the *ab initio* ones presented in Fig. 1. After a transient behavior for small ℓ , all the curves with varying α approach a constant, indicating not only that the universal leading logarithmic term in S_α is correctly described by RSP, but the finite-size corrections are also. In the range of α considered in the figure, we find that the additive constant is well described by

$$S_\alpha \approx S_\alpha^{\text{RSP}} + \frac{a}{\alpha} + b + o(1), \quad (27)$$

where the disorder-dependent constants a and b in the case of random disorder take the values $a \approx 0.61$ and $b \approx -0.47$.

B. Finite-size effects

Having established the correctness of the asymptotic RSRG results for S_α in the region $1 \ll \ell \ll L$, we can consider the finite-size effects. One of the most remarkable result of

conformal invariance is that the finite-size scaling is obtained with the replacement

$$\ell \rightarrow \frac{L}{\pi} \sin\left(\frac{\pi \ell}{L}\right), \quad (28)$$

in the thermodynamic limit result. The right-hand side (rhs) of the above equation is known as a chord length. However, when conformal invariance is broken, the chord length does not give the finite-size scaling. In fact, using the results reported previously it is easy to show that this is the case, as it was already shown for some random Ising systems.⁴⁵

Even if conformal invariance is broken, scale invariance still holds. Thus the finite-size scaling can always be taken into account by the substitution

$$\ell \rightarrow \frac{L}{\pi} Y\left(\frac{\pi \ell}{L}\right). \quad (29)$$

The great predictive power of conformal symmetry is that independently of the observable (but built with primary operators) the scaling function is always $Y(x) = \sin(x)$, while in general scale-invariant theories the function $Y(x)$ *does depend on the observable*. Some results on the finite-size scaling of entanglement in 1D critical nonconformal systems have been already reported.^{45–48} The function $Y(x)$ for S_α must, however, satisfy simple symmetry constraints. First, S_α is symmetric for $\ell \rightarrow L - \ell$, thus $Y(x) = Y(\pi - x)$. Second, periodic boundary conditions require S_α to be a periodic function of ℓ of period L , and so $Y(x) = Y(\pi + x)$. Thus we can expand $Y(x)$ in Fourier modes as

$$Y(x) = \left[1 + \sum_{j=1}^{\infty} k_j \right] \sin x - \sum_{k=1}^{\infty} \frac{k_j}{2j+1} \sin((2j+1)x), \quad (30)$$

where we also imposed $Y(x \ll 1) \sim x$ to reproduce the correct thermodynamic limit. The chord length has only the first mode and so corresponds to $k_j = 0$ for any j . This expansion in terms of Fourier modes is particularly useful because we expect that the contribution of the first few modes will be enough to have a reasonable approximation of the scaling function $Y(x)$. Indeed, Fig. 3 shows that only the first term k_1 is enough to describe accurately the observed behavior for the RSP entanglement entropy

$$\begin{aligned} Y(x) &\simeq (1 + k_1) \sin x - \frac{k_1}{3} \sin 3x \\ &= \sin x \left[1 + \frac{4}{3} k_1 \sin^2 x \right], \end{aligned} \quad (31)$$

with $k_1 \approx 0.115$. The obtained scaling function in the presence of disorder is greater than the chord length.

Figure 2 shows that the finite-size scaling in the *ab initio* calculations is equivalent to the RSP ones (or else for $\ell \sim L$ the various curves should bend). This means that the finite-size scaling of all S_α in the spin chain is described by Eq. (31), as we also checked directly.

C. Probability distribution of the Rényi entropy

The disorder-averaged Rényi entropy S_α gives only access to the averaged number of the in-out singlets while \hat{S}_α gives access to the full in-out singlets distribution $P(n)$

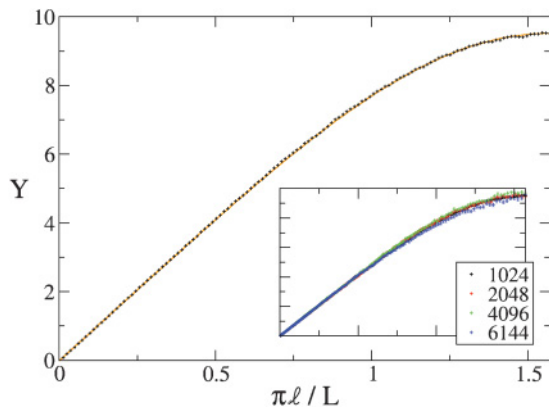


FIG. 3. (Color online) The finite-size scaling function for the entanglement entropy $Y(x)$ in Eq. (29). Main: RSP data averaged over 1 440 000 disorder realizations for $L = 1024$. The continuous (red) curve is the proposed phenomenological formula (31) describing perfectly the data points. Inset: The same plot for different values of L showing the collapse on a single scaling function.

(i.e., the probability distribution of the R enyi entropy and so to the full entanglement spectrum). Indeed \hat{S}_α is related to the cumulant-generating function $g(t)$ of the in-out singlets distribution by Eq. (16).

We first consider the RSP data because they allow to explore larger system sizes. Only after having established the asymptotic behavior will we consider *ab initio* data and show consistency with the proposed scaling.

We observed that the R enyi entropies S_α^{RSP} do not have subleading corrections depending on the parity of the block, making the asymptotic analysis quite straightforward. Oppositely, the data for $\hat{S}_\alpha^{\text{RSP}}$ (see Fig. 4) show that they depend on the block parity in a way similar to clean systems.⁴² To analyze the numerical data we conjecture the following asymptotic behavior

$$\hat{S}_\alpha^{\text{RSP}}(\ell) \approx A_t S_\alpha^{\text{RSP}}(\ell) + B_t \ln 2 - (-1)^\ell f_t [S_\alpha^{\text{RSP}}(\ell)] \ln 2, \quad (32)$$

where t is defined in Eq. (17). A_t and B_t are the two functions introduced in Eq. (23), while f_t takes into account the corrections to the scaling and goes to 0 for $\ell \rightarrow \infty$. The form of the corrections is inspired by the results in clean systems, while the leading term is the solution asymptotic $g(t)$ in Eqs. (23) and (24). In the top of Fig. 4 we also report the RSRG value for A_t that seems to be in qualitative agreement with the numerical data. A full quantitative description requires the elimination of the corrections to the scaling.

To provide an unbiased description of the asymptotic behavior of \hat{S}_α , we define the functions $s_\alpha^{\text{even}}(\ell)$ and $s_\alpha^{\text{odd}}(\ell)$ from the interpolation relative to even and odd blocks, respectively. We can isolate the leading behavior of $\hat{S}_\alpha^{\text{RSP}}$ by considering the average over the two interpolating functions, that is,

$$\hat{S}_\alpha^{eo}(\ell) \equiv \frac{s_\alpha^{\text{even}}(\ell) + s_\alpha^{\text{odd}}(\ell)}{2}. \quad (33)$$

This definition eliminates the leading corrections to the scaling. In fact, in the lower panel of Fig. 4 we have a linear relation between \hat{S}_α^{eo} and S_α^{RSP} for all reported values of α

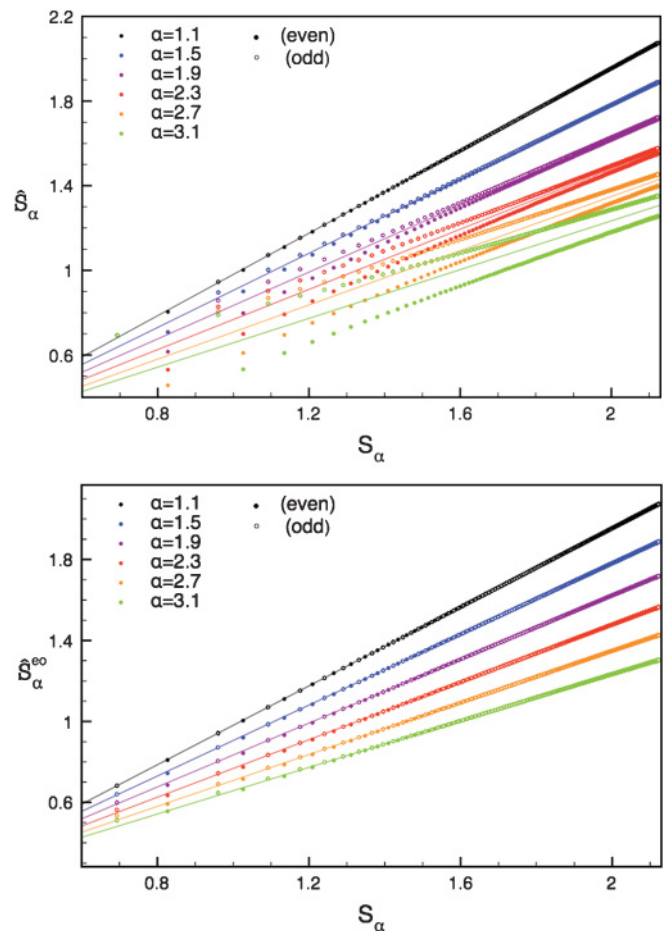


FIG. 4. (Color online) Top: RSP results for \hat{S}_α as a function of S_α for a chain of 1024 spins and 1 440 000 disorder realizations. Bottom: Even-odd average of \hat{S}_α eliminating leading corrections to the scaling. In both panels the continuous lines are the analytic RSRG result for A_t .

(while the nonaveraged data in the top panel are linear only for α close to 1).

From this linear dependence we can extract the functions A_t and B_t using the RSRG relation

$$\hat{S}_\alpha^{eo} \simeq A_t S_\alpha^{\text{RSP}}(\ell) + \ln 2 B_t. \quad (34)$$

The resulting values for the universal coefficient $A_{t(\alpha)}$ for $\alpha \leq 10$ and for $L = 1024$ and $L = 10\,000$ are reported in Fig. 5. For small α (≤ 3.5) there are negligible finite-size corrections and the data perfectly agree with the RSRG result in Eq. (24), showing the predictive power of the RSRG to determine A_t . For larger α , finite-size corrections are important and indeed the data differ from the analytical prediction, but the larger system sizes are closer. We believe that in the thermodynamic limit the RSRG A_t describes the correct behavior for any α . The reason for these finite-size effects is also easily understood: The asymptotic formula is valid for \hat{S}_α large, while in this region of α we have $\hat{S}_\alpha \sim 1$. Even if not asymptotic, the large α results show an interesting behavior: Independently of L , they follow a $-1/t$ behavior (see inset in Fig. 5), typical of a Poissonian distribution of singlets. The reason for this Poissonian behavior can be traced back to the fact that for $t \rightarrow -\infty$ we are giving a large weight to

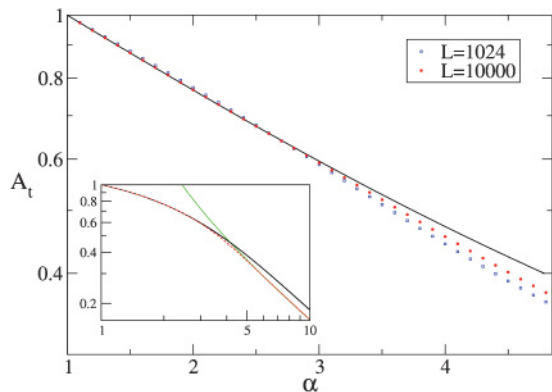


FIG. 5. (Color online) The universal constant A_t obtained from RSP data for $L = 1024$ (1,440,000 disorder realizations) and $L = 10\,000$ (320 000 realizations). Main plot: For $\alpha \leq 3.5$ finite-size effects are negligible and the RSRG prediction (continuous line) describes the data. Inset: Crossover to the nonuniversal Poissonian behavior (green continuous line) for larger α .

short-range singlets that are produced almost independently. Little weight is instead given to long-range singlets responsible for the universal physics and so for these values of α and L we are probing the uv physics. According to this interpretation, a crossover from the universal behavior of Eq. (24) to a uv Poissonian behavior always takes place for $\alpha \sim \ln L$, in agreement with Fig. 5.

We can now move to the *ab initio* calculation to check the validity of the RSP scenario for \hat{S}_α . As before, we focus on the relation between \hat{S}_α and S_α and, in particular, on the universal slope of the linear relation between them. The results are reported in Fig. 6. Asymptotically, the slopes of these curves tend to the RSRG prediction for A_t shown as continuous lines in the figure. Also the finite-size scaling scaling is well described by Eq. (31), as evident from the fact that the linear relation between \hat{S}_α and S_α is correct even for large values of ℓ (i.e., of S_α) in the various plots. However, as clear by a visual comparison between Figs. 6 and 4 (top), the constant term in this relation is different [and both different from the analytic B_t in Eq. (24)]. The degree of universality of this term is discussed in the next section.

Having established the correct asymptotic behavior we can consider the oscillating corrections to the scaling defined in Eq. (32). The numerical estimate of $f_t(S)$ can be obtained as

$$f_t(S) \simeq \frac{s_\alpha^{\text{odd}}(\ell) - s_\alpha^{\text{even}}(\ell)}{2} + \dots, \quad (35)$$

where the dots denote subsubleading terms (we recall that $s_\alpha^{\text{odd/even}}$ are interpolations and so defined for any ℓ). The data obtained in this way are reported in Fig. 7. The linear behavior in log-scale shows that for $\alpha \leq 5$ (for larger α further subsubleading corrections must be considered)⁴² $f_t(S_\alpha)$ decays exponentially

$$f_t(x) = F_t e^{-\nu_t x}, \quad (36)$$

(i.e., a power-law correction in ℓ). $\nu_{t(\alpha)}$ is a new universal critical exponent governing the corrections to the scaling of \hat{S}_α , analogous to the one introduced in clean systems.^{42,43} We can see that $\nu_{t(\alpha)}$ decreases with increasing α , but a

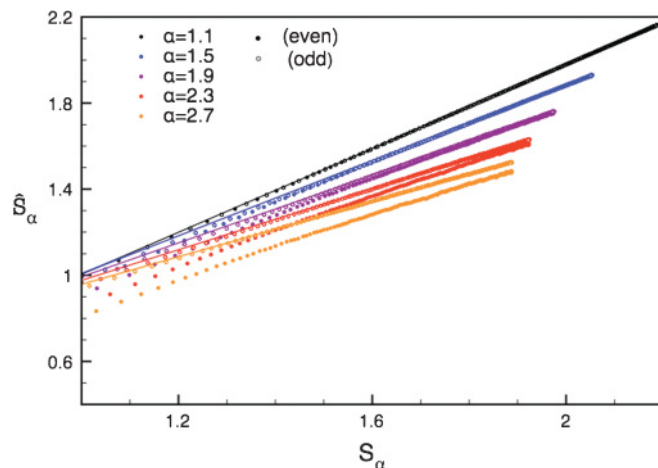


FIG. 6. (Color online) *Ab initio* \hat{S}_α as a function of S_α for a spin-chain of 1024 spins and 73 000 disorder realizations. The continuous lines represent the RSRG prediction for the slope. The additive terms are different from those in Fig. 4.

precise numerical estimate is difficult. For clean systems it has been shown^{42,43} that $\nu_{t(\alpha)} = 2K/\alpha$ with K an α -independent exponent equal to the scaling dimension of a relevant operator. We can rule out this form for the random spin chain, but the accuracy of our results does not allow to establish numerically an exact formula for the α dependence of the exponent. We also mention that the corrections to the scaling are of the same form also in *ab initio* calculations, as is qualitatively clear from Fig. 6 and quantitatively checked but not reported here. This shows the correctness of the RSP description and also that the real spin chain does not introduce new leading corrections to the scaling in addition to the RSP ones.

D. Universality

All the results presented until now, both *ab initio* and RSP, have been obtained for random distributions of the coupling constant J in the interval $[0,1]$. However, the universal prediction of RSRG must be independent of the distributions

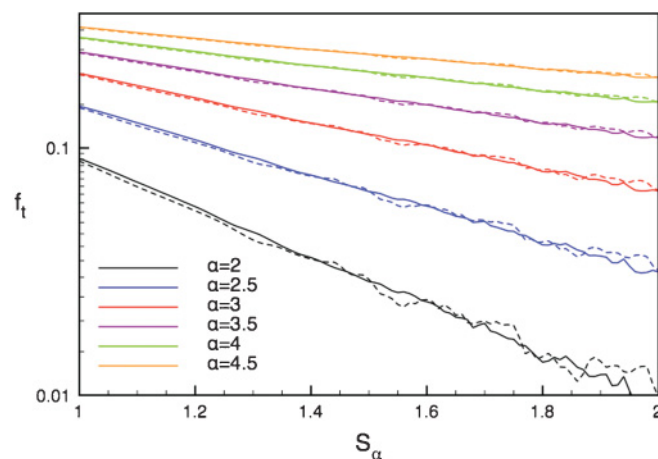


FIG. 7. (Color online) Scaling functions for the correction to the scaling $f_t(S)$ in Eq. (32) obtained as the difference of $s_\alpha^{\text{odd}}(\ell)$ and $s_\alpha^{\text{even}}(\ell)$. Full and dashed lines correspond to uniform and exponential distributions of disorder, respectively.

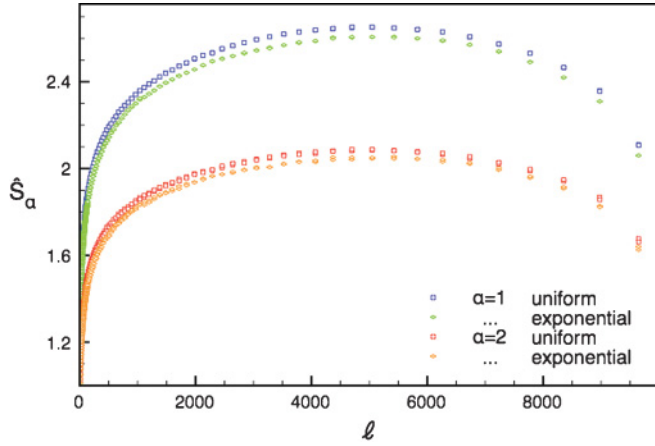


FIG. 8. (Color online) \hat{S}_α for two disorder distributions. The RSP data are for chains of 10 000 spins and averaged over 320 000 configurations.

of J (as long as new symmetries are not introduced). We check this universality by studying the RSP chain with $L = 10\,000$ spins with coupling distributed both uniformly $J \in [0, 1]$ and exponentially $P(J) \sim e^{-J}$. In Fig. 8 we report the numerical RSP results of \hat{S}_α for $\alpha = 1, 2$ for the two distributions of the disorder. As expected, the two distributions lead to slightly different results: Only the leading logarithmic term in ℓ is universal while the additive constant term is not.

To check the universality of the leading term, Fig. 9 reports \hat{S}_α as a function S_α for $\alpha = 2.9$ (other values of α lead to equivalent plots) for the two distributions. The two curves perfectly coincide, despite the fact that when they are plotted as a function of ℓ they are different. This means that all the nonuniversal behavior of the additive constants is washed out and we are left with a universal function. At first this result can seem surprising, but it is easy to realize that, in this kind of plot, the dependence on the nonuniversal cutoff or lattice scale a disappears and the leftover difference of nonuniversal additive constants is universal. For example, for the conformal

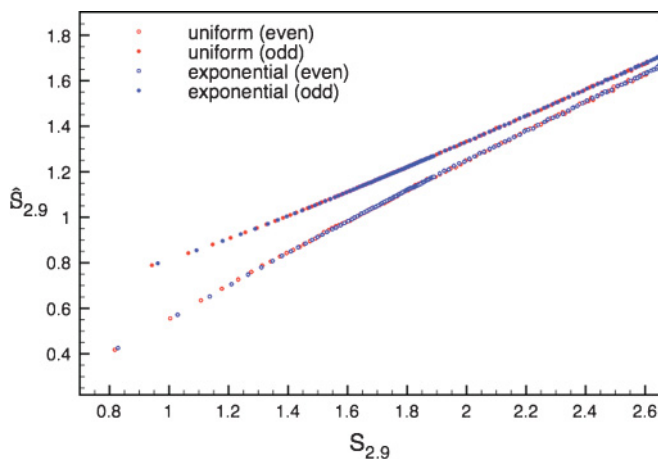


FIG. 9. (Color online) \hat{S}_α as function of S_α for $\alpha = 2.9$ and for two disorder distributions (RSP data with $L = 10\,000$ and 320 000 configurations). The scaling function is disorder independent.

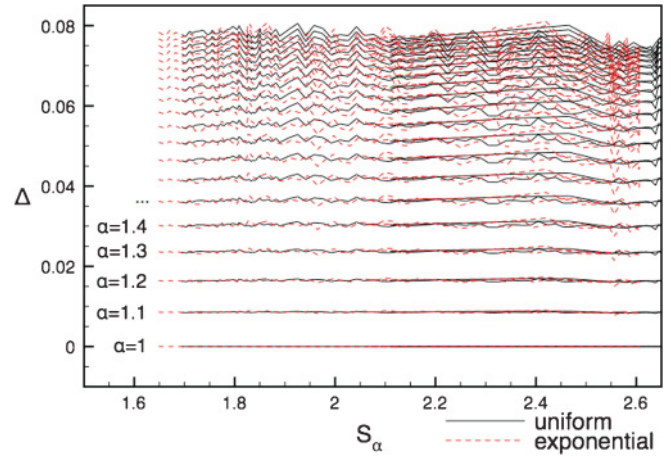


FIG. 10. (Color online) The quantity Δ defined in Eq. (38) vs S_α for uniform and exponential distributions of disorder. With varying α the two differences are the same, showing the universality of the coefficient $B_{t(\alpha)}$.

entropies (14) we have the *universal* relation

$$S_\alpha^{CFT} = \frac{S_{VN}^{CFT}}{2} \left(1 + \frac{1}{\alpha}\right) + c'_\alpha - \frac{c'_1}{2} \left(1 + \frac{1}{\alpha}\right), \quad (37)$$

where evidently all the a dependence disappeared. To our knowledge, this property has not been explored at all in clean systems, but one can easily check that in the exact results for the critical XY model⁴⁹ the dependence on the irrelevant parameter γ disappears in Eq. (37).

Having established that both A_t and B_t are universal, we reconsider our results for the disordered systems. We already discussed for the uniform distribution (see Fig. 5) how the numerical value of A_t agrees with the analytical RSRG prediction. The independence of A_t on the disorder distribution confirms its universality. In Fig. 10, we plot the quantity

$$\Delta = \hat{S}_\alpha^{eo} - \frac{g_\mu[t(\alpha)]}{1 - \alpha}, \quad (38)$$

where $g_{(\mu)}(t)$ is the function in Eq. (22) and μ is fixed by S_α via $\mu = \frac{3}{\ln 2} S_\alpha + \frac{1}{3}$. This quantity has been built in such a way as to cancel the leading behavior A_t thus leaving only B_t . Albeit a little noisy, Fig. 10 shows clearly the disorder independence of B_t .

Disappointingly, as shown for uniform disorder, we found that the RSP and *ab initio* calculation for \hat{S}_α provide different values for the constant $B_{t(\alpha)}$ that are both different from the RSRG expression in Eq. (24). On one hand, this is showing that the RSP description is unable to catch this feature of the spin chain because numerical RSP and *ab initio* data disagree. On the other hand, this is also showing that while carrying out the analytic results for $g(t)$, some of the assumptions made influence significantly this quantity. There are two possible explanations to motivate the last discrepancy. One is that the distribution $f(\mu)$ in Eq. (18) contains some additional (subleading) terms not considered here. In fact, as already discussed, Eq. (18) has been deduced neglecting terms coming from the starting disorder distribution and it is only asymptotically true. The other possibility is, instead, that the discarded terms in the renewal equation (19) contribute to

B_t . Several pieces of information have been indeed ignored there: memory beyond first order, multiple decimations, the flow of the distribution to the critical point, and so on. We found it rather improbable that $f(\mu)$ should be modified. It is difficult to imagine how to modify it keeping all the other correct results (i.e., the entanglement entropy, A_t , etc.). On the other hand, solving the renewal equation in the presence of the discarded effects is very hard (maybe impossible). Thus, to convince oneself that these processes can be responsible for a changing in B_t , we tried to add some oversimplified processes (but physically motivated) to the renewal equation: We found that all these processes change B_t , but leave A_t unchanged, showing that this is the most probable explanation of the discrepancy. However, from the *ab initio* results, we know that the real spin chain introduces further corrections to this term and so we do not find it reasonable to embark in a difficult calculation that, in any case, will not provide the correct answer for the spin chain.

To conclude the universality section, it is worth mentioning that the oscillating corrections to the scaling [the function f_t in Eq. (32)] also does not depend on the disorder distribution as shown in Fig. 7, confirming their universality.

V. CONCLUSION

We provided an analytical and numerical description of the Rényi entropies S_α and \hat{S}_α in an RSP. For S_α the leading logarithmic behavior is α independent and only the subleading constant term depends on α

$$S_\alpha = \frac{1}{1-\alpha} \overline{\ln \text{Tr}[\rho^\alpha]} \simeq \frac{\ln 2}{3} \ln \ell + d'_\alpha. \quad (39)$$

The leading universal term has been determined analytically while the nonuniversal correction d'_α only numerically. Oppositely, the leading universal term of \hat{S}_α has a nontrivial α dependence. Its scaling behavior can be written in a completely *universal* form as

$$\hat{S}_\alpha = \frac{1}{1-\alpha} \ln \overline{\text{Tr}[\rho^\alpha]} \simeq A_{(1-\alpha)\ln 2} S_\alpha + B_{(1-\alpha)\ln 2}. \quad (40)$$

Indeed, we pointed out that the functions A_t and b_t connecting linearly \hat{S}_α and S_α are both independent of the cutoff length introduced by the chain and so are universal. The analytic result based on the solution of RSRG equations agrees perfectly with the numerical data as shown in Fig. 5, giving a full characterization of the asymptotic behavior. Instead a first-order RG prediction for the subleading term B_t disagrees with the numerical data. We showed evidence that this disagreement should be related to the approximations done in the RG equations. Only an improved, but much more difficult (and maybe impossible) calculation can provide the exact result for B_t .

We showed [Eq. (21)] that the Rényi entropies \hat{S}_α are simply related to the Laplace transform of the singlet distribution function. Thus the measure of \hat{S}_α can be used to directly calculate the singlet distribution function, from which any universal quantity in the RSP can be deduced. We then conclude that the knowledge of only the leading order of \hat{S}_α is enough to full characterize this kind of disorder system while in the conformal invariant critical point the leading piece of the entanglement spectrum only gives the central charge and no information about the operator content (that can be accessed, in part, by looking at subleading corrections^{42,43} and fully by looking at the entanglement of disjoint intervals).⁴¹

We also studied the finite-size scaling: For finite chains the previous relations still hold if the subsystem length ℓ is replaced by a *modified chord length* that is phenomenologically well approximated by Eq. (31). We do not have a theoretical explanation for this finite-size scaling form.

Assuming that the random-singlet description is equally valid for the random Heisenberg model, as is plausible and often assumed but not yet proved or firmly confirmed numerically, then we are in the surprising situation of knowing the entanglement spectrum exactly for the random Heisenberg model, but only approximately for the corresponding pure model (apart from some exact results for small ℓ).⁵⁰

ACKNOWLEDGMENTS

J.E.M. acknowledges support from NSF DMR-0804413.

¹L. Amico, R. Fazio, A. Osterloh, and V. Vedral, *Rev. Mod. Phys.* **80**, 517 (2008); J. Eisert, M. Cramer, and M. B. Plenio, *ibid.* **82**, 277 (2010); *Entanglement entropy in extended systems*, P. Calabrese, J. Cardy, and B. Doyon Eds, *J. Phys. A* **42**, 500301 (2009).

²C. Holzhey, F. Larsen, and F. Wilczek, *Nucl. Phys. B* **424**, 443 (1994).

³G. Vidal, J. I. Latorre, E. Rico, and A. Kitaev, *Phys. Rev. Lett.* **90**, 227902 (2003); J. I. Latorre, E. Rico, and G. Vidal, *Quantum Inf. Comput.* **4**, 048 (2004).

⁴P. Calabrese and J. Cardy, *J. Stat. Mech.* (2004) P06002.

⁵P. Calabrese and J. Cardy, *J. Phys. A* **42**, 504005 (2009).

⁶I. Peschel, M. Kaulke, and O. Legeza, *Ann. Phys. (Leipzig)* **8**, 153 (1999); M.-C. Chung and I. Peschel, *Phys. Rev. B* **64**, 064412 (2001); I. Peschel, *J. Stat. Mech.* (2004) P06004.

⁷P. Calabrese and A. Lefevre, *Phys. Rev. A* **78**, 032329 (2008).

⁸F. Pollmann and J. E. Moore, *New J. Phys.* **12**, 025006 (2010).

⁹F. Franchini, A. R. Its, V. E. Korepin, and L. A. Takhtajan, e-print arXiv:1002.2931.

¹⁰L. Tagliacozzo, T. R. de Oliveira, S. Iblisdir, and J. I. Latorre, *Phys. Rev. B* **78**, 024410 (2008).

¹¹F. Pollmann, S. Mukerjee, A. M. Turner, and J. E. Moore, *Phys. Rev. Lett.* **102**, 255701 (2009).

¹²H. Li and F. D. M. Haldane, *Phys. Rev. Lett.* **101**, 010504 (2008).

¹³N. Regnault, A. B. Bernevig, and F. D. M. Haldane, *Phys. Rev. Lett.* **103**, 016801 (2009).

¹⁴A. M. Läuchli, E. J. Bergholtz, J. Suorsa, and M. Haque, *Phys. Rev. Lett.* **104**, 156404 (2010).

¹⁵M. Levin and X.-G. Wen, *Phys. Rev. Lett.* **96**, 110405 (2006).

¹⁶A. Kitaev and J. Preskill, *Phys. Rev. Lett.* **96**, 110404 (2006).

¹⁷M. Haque, O. Zozulya, and K. Schoutens, *Phys. Rev. Lett.* **98**, 060401 (2007); O. S. Zozulya, M. Haque, K. Schoutens, and E. H. Rezayi, *Phys. Rev. B* **76**, 125310 (2007); O. S. Zozulya, M. Haque, and N. Regnault, *ibid.* **79**, 045409 (2009).

- ¹⁸E. Fradkin and J. E. Moore, *Phys. Rev. Lett.* **97**, 050404 (2006); B. Hsu, M. Mulligan, E. Fradkin, and E. A. Kim, *Phys. Rev. B* **79**, 115421 (2009); J. M. Stèphan, S. Furukawa, G. Misguich, and V. Pasquier, *ibid.* **80**, 184421 (2009); E. Fradkin, *J. Phys. A* **42**, 504011 (2009); B. Hsu and E. Fradkin, *J. Stat. Mech.* (2010) P09004; J. M. Stèphan, G. Misguich, and V. Pasquier, *Phys. Rev. B* **82**, 125455 (2010); M. Oshikawa, e-print arXiv:1007.3739.
- ¹⁹V. Popkov and M. Salerno, *Phys. Rev. E* **82**, 011142 (2010).
- ²⁰D. S. Fisher, *Phys. Rev. B* **50**, 3799 (1994).
- ²¹D. S. Fisher, *Phys. Rev. B* **51**, 6411 (1995).
- ²²K. Damle, O. Motrunich, and D. A. Huse, *Phys. Rev. Lett.* **84**, 3434 (2000).
- ²³S. K. Ma, C. Dasgupta, and C. K. Hu, *Phys. Rev. Lett.* **43**, 1434 (1979).
- ²⁴G. Refael and J. E. Moore, *Phys. Rev. Lett.* **93**, 260602 (2004).
- ²⁵N. Laflorencie, *Phys. Rev. B* **72**, 140408 (2005).
- ²⁶G. De Chiara, S. Montangero, P. Calabrese, and R. Fazio, *J. Stat. Mech.* (2006) P03001.
- ²⁷G. Refael and J. E. Moore, *Phys. Rev. B* **76**, 024419 (2007).
- ²⁸G. Refael and J. E. Moore, *J. Phys. A* **42**, 404010 (2009).
- ²⁹C. Tsallis, *J. Stat. Phys.* **52**, 479 (1988).
- ³⁰I. J. Cirac and G. Sierra, *Phys. Rev. B* **81**, 104431 (2010).
- ³¹A. B. Zamolodchikov, *JETP Lett.* **43**, 731 (1986) [*Pisma Zh. Eksp. Teor. Fiz.* **43**, 565 (1986)].
- ³²R. Santachiara, *J. Stat. Mech.* (2006) L06002; D. Binosi, G. De Chiara, S. Montangero, and A. Recati, *Phys. Rev. B* **76**, 140405(R) (2007).
- ³³L. Fidkowski, H.-H. Lin, P. Titum, and G. Refael, *Phys. Rev. B* **79**, 155120 (2009); L. Fidkowski, G. Refael, N. Bonesteel, and J. E. Moore, *ibid.* **78**, 224204 (2008).
- ³⁴F. Gliozzi and L. Tagliacozzo, *J. Stat. Mech.* (2010) P01002; M. A. Metlitski, C. A. Fuertes, and S. Sachdev, *Phys. Rev. B* **80**, 115122 (2009).
- ³⁵I. Peschel, *J. Phys. A* **36**, L205 (2003); J. I. Latorre and A. Riera, *ibid.* **42**, 504002 (2009); I. Peschel and V. Eisler, *ibid.* **42**, 504003 (2009).
- ³⁶A. Saguia and M. S. Sarandy, *Phys. Lett. A* **374**, 3384 (2010).
- ³⁷I. Affleck and A. W. W. Ludwig, *Phys. Rev. Lett.* **67**, 161 (1991).
- ³⁸H.-Q. Zhou, T. Barthel, J. O. Fjærerstad, and U. Schollwoeck, *Phys. Rev. A* **74**, 050305 (2006); N. Laflorencie, E. S. Sorensen, M.-S. Chang, and I. Affleck, *Phys. Rev. Lett.* **96**, 100603 (2006); E. S. Sorensen, N. Laflorencie, and I. Affleck, *J. Phys. A* **42**, 504009 (2009).
- ³⁹M. Fagotti *et al.*, (unpublished).
- ⁴⁰M. Fagotti and P. Calabrese, *J. Stat. Mech.* (2010) P04016.
- ⁴¹M. Caraglio and F. Gliozzi, *J. High Energy Phys.* **11** (2008) 076; S. Furukawa, V. Pasquier, and J. Shiraishi, *Phys. Rev. Lett.* **102**, 170602 (2009); P. Calabrese, J. Cardy, and E. Tonni, *J. Stat. Mech.* (2009) P11001; H. Casini and M. Huerta, *J. High Energy Phys.* **03** (2009) 048; V. Alba, L. Tagliacozzo, and P. Calabrese, *Phys. Rev. B* **81**, 060411 (2010); F. Iglói and I. Peschel, *Europhys. Lett.* **89**, 40001 (2010); H. Casini, *J. Stat. Mech.* (2010) P08019; P. Calabrese, *ibid.* (2010) P09013; M. Headrick, *Phys. Rev. D* **82**, 126010 (2010); P. Calabrese, J. Cardy, and E. Tonni, *J. Stat. Mech.* (2011) P01021.
- ⁴²P. Calabrese, M. Campostrini, F. Essler, and B. Nienhuis, *Phys. Rev. Lett.* **104**, 095701 (2010); P. Calabrese and F. H. L. Essler, *J. Stat. Mech.* (2010) P08029.
- ⁴³J. Cardy and P. Calabrese, *J. Stat. Mech.* (2010) P04023; P. Calabrese, J. Cardy, and I. Peschel, *ibid.* (2010) P09003; E. Ercolessi, S. Evangelisti, F. Franchini, and F. Ravanini, e-print arXiv:1008.3892.
- ⁴⁴A. B. Kallin, I. González, M. B. Hastings, and R. Melko, *Phys. Rev. Lett.* **103**, 117203 (2009); **104**, 157201 (2010); J. C. Xavier, *Phys. Rev. B* **81**, 224404 (2010); H. F. Song, S. Rachel, and K. Le Hur, *ibid.* **82**, 012405 (2010); F. Alet, I. P. McCulloch, S. Capponi, and M. Mambrini, *ibid.* **82**, 094452 (2010); M. Fagotti and P. Calabrese, *J. Stat. Mech.* (2011) P01017.
- ⁴⁵F. Iglói and Y.-C. Lin, *J. Stat. Mech.* (2008) P06004.
- ⁴⁶V. Popkov and M. Salerno, *Phys. Rev. A* **71**, 012301 (2005); V. Popkov, M. Salerno, and G. Schuetz, *ibid.* **72**, 032327 (2005).
- ⁴⁷F. C. Alcaraz and V. Rittenberg, *J. Stat. Mech.* (2010) P03024; F. C. Alcaraz, V. Rittenberg, and G. Sierra, *Phys. Rev. E* **80**, 030102(R) (2009).
- ⁴⁸M. Campostrini and E. Vicari, *J. Stat. Mech.* (2010) P08020.
- ⁴⁹I. Peschel, *J. Stat. Mech.* (2004) P12005; A. R. Its, B.-Q. Jin, and V. E. Korepin, *J. Phys. A* **38**, 2975 (2005); F. Franchini, A. R. Its, and V. E. Korepin, *ibid.* **41**, 025302 (2008); F. Iglói and R. Juhasz, *Europhys. Lett.* **81**, 57003 (2008).
- ⁵⁰J. Sato and M. Shiroishi, *J. Phys. A* **40**, 8739 (2007); J. Damerau, F. Göhmann, N. P. Hasencllever, and A. Klümper, *ibid.* **40**, 4439 (2007); J. Sato, M. Shiroishi, and M. Takahashi, *J. Stat. Mech.* (2006) P12017; B. Nienhuis, M. Campostrini, and P. Calabrese, *ibid.* (2009) P02063; L. Bianchi, F. Colomo, and P. Verrucchi, *Phys. Rev. A* **80**, 022341 (2009); V. Alba, M. Fagotti, and P. Calabrese, *J. Stat. Mech.* (2009) P10020.